GPI-anchored Influenza Hemagglutinin Induces Hemifusion to both Red Blood Cell and Planar Bilayer Membranes

Grigory B. Melikyan,* Judith M. White,‡ and Fredric S. Cohen*

*Department of Molecular Biophysics and Physiology, Rush Medical College, Chicago, Illinois 60612; and‡Department of Cell Biology, University of Virginia Health Sciences Center, Charlottesville, Virginia 22908

Abstract. Under fusogenic conditions, fluorescent dye redistributed from the outer monolayer leaflet of red blood cells (RBCs) to cells expressing glycophosphatidylinositol-anchored influenza virus hemagglutinin (GPI-HA) without transfer of aqueous dye. This suggests that hemifusion, but not full fusion, occurred (Kemble, G. W., T. Danieli, and J. M. White. 1994. *Cell.* 76:383–391). We extended the evidence for hemifusion by labeling the inner monolayer leaflets of RBCs with FM4-64 and observing that these inner leaflets did not become continuous with GPI-HA–expressing cells. The region of hemifusion-separated aqueous contents, the hemifusion diaphragm, appeared to be extended and was long-lived. But when RBCs hemifused to GPI-HA–expressing cells were osmotically swollen, some diaphragms were disrupted, and spread of both inner leaflet and aqueous dyes was observed. This was characteristic of full fusion: inner leaflet and aqueous probes spread to cells expressing wild-type HA (wt-HA). By simultaneous video fluorescence microscopy and time-resolved electrical admittance measurements, we rigorously demonstrated that GPI-HA–expressing cells hemifuse to planar bilayer membranes: lipid continuity was established without formation of fusion pores. The hemifusion area became large. In contrast, for cells expressing wt-HA, before lipid dye spread, fusion pores were always observed, establishing that full fusion occurred. We present an elastic coupling model in which the ectodomain of wt-HA induces hemifusion and the transmembrane domain, absent in the GPI-HA–expressing cells, mediates full fusion.

Hemagglutinin (HA)[1] of influenza virus is the best characterized fusion protein (Wiley and Skehel, 1987; White, 1992). Influenza virus enters the cell's endocytotic pathway. Exposed to the low pH of endosomes, HA undergoes conformational changes that lead to fusion. The structure of HA is known in its nonfusogenic form at neutral pH (Wilson et al., 1981). There is also crystallographic (Bullough et al., 1994), spectroscopic, morphological (Wharton et al., 1995), and biochemical data on the conformational changes HA undergoes to its fusogenic form at acidic pH (for reviews see Steinhauer et al., 1992; Doms, 1993; Stegmann and Helenius, 1993). However, the relation of specific changes to fusion is still poorly understood (White, 1994). Also the mechanism by which HA or any other proteins induce fusion—the joining of formerly distinct aqueous compartments by the coalescence of two lipid bilayer membranes into one—is not yet known.

An approach to elucidate the fusion mechanism is to identify fusion intermediates. Recently, cells, referred to as BHA-PI cells, have been generated that express on their surfaces the ectodomain of HA, linked to glycosylinositol phospholipid (GPI-HA) (Kemble et al., 1993). This anchors it to the outer leaflets (monolayers) of cell membranes. Under fusogenic conditions lipid probes introduced into the outer leaflets of RBCs move into BHA-PI cell membranes without transfer of aqueous dyes (Kemble et al., 1994). These are the results one would expect if GPI-HA causes hemifusion, but not full fusion. However, these findings are not sufficient to be certain that full fusion did not take place, or that hemifusion did indeed happen. As discussed (Kemble et al., 1994), a transient, local structure rather than a stable single lipid bilayer shared by the cells could have temporarily connected the BHA-PI cell and RBC membranes, allowing the observed spread of lipid dye. Furthermore, fusion pores might have formed either too small or too short lived to allow passage of aqueous fluorescent dyes, in which case fusion would have occurred undetected.

Address all correspondence to Fredric S. Cohen, Department of Molecular Biophysics and Physiology, Rush Medical College, 1653 W. Congress Parkway, Chicago, IL 60612. Tel.: (312) 942-6753. Fax: (312) 942-8711.

1. *Abbreviations used in this paper*: BHA, water-soluble HA ectodomain obtained by bromelain cleavage; BHA-PI, cells expressing GPI-HA; CF, 6-carboxyfluorescein; DiI, 1,1′-dihexadecyl-3,3,3′3′-tetramethyl indocarbocyanine perchlorate; DOPE, dioleoylphosphatidylethanolamine; Eth, ethidium bromide; GPI, glycosylphosphatidylinositol; GPI-HA, HA ectodomain linked to GPI; HA, hemagglutinin; HA-WT, cells expressing wild-type HA; R18, octadecylrhodamine B; rhoPE, lissamine rhodamine B sulfonyl–labeled DOPE; TM, transmembrane domain of HA; wt, wild type; wt-HA, cells expressing wild-type HA.

If hemifusion occurs, the contacting monolayer leaflets of opposing membranes would merge and would be cleared from the region of contact. The noncontacting leaflets of each membrane would not join each other, remaining distinct, but would come into direct apposition. This would result in a single shared bilayer, referred to as a hemifusion diaphragm, that would continue to separate aqueous compartments. Fusion would be completed only when fusion pores were created within the diaphragm, which would establish aqueous continuity. Thus, three criteria should be satisfied before concluding that hemifusion has occurred. First, the outer leaflets of membranes must become continuous. Second, the inner leaflets do not become continuous, but rather must remain intact. Third, fusion pores must not form.

In this paper we use fluorescence measurements to follow movement of aqueous and membrane dyes and electrophysiological techniques to detect small fusion pores. We establish that BHA-PI cells hemifuse to target membranes by showing that the above three criteria are met. We introduce a novel fluorescence approach to demonstrate that the inner leaflets of RBCs and BHA-PI cells do not become continuous, but that the outer leaflets do. Simultaneous fluorescence and electrical measurements were used to prove that lipid dye spreads between BHA-PI cells and planar bilayer membranes without formation of any fusion pores. We also probed the structure that provided the lipid continuity: for both RBCs and planar bilayers as target, the connecting structure appears to be extended, and is long lasting. Thus, for these systems hemifusion occurs and the hemifused diaphragms are long-lived structures. It follows that, as proposed (Kemble et al., 1994), the transmembrane and perhaps the cytosolic domain of HA, absent in GPI-HA, are required for complete fusion.

Materials and Methods

HA-expressing Cells

CHO-K1 cells expressing either X:31 influenza HA (referred to as HA-WT) or expressing the GPI-linked ectodomain of X:31 HA (BHA-PI) were maintained as described (Kemble et al., 1993, 1994). Cells were grown in glutamine-deficient MEM (GIBCO BRL, Gaithersburg, MD) with 10% supplemented calf serum (Hyclone Laboratories, Logan, UT) and 400 μM L-methionine sulfoximine (MSX; Sigma Chemical Co., St. Louis, MO). The medium for BHA-PI cells also contained 250 μM 1-deoxymannojirimycin (dMM; Calbiochem-Novabiochem Corp., LaJolla, CA) to prevent terminal oligosaccharide processing, thereby preserving receptor binding activity of GPI-linked HA.

Labeling Outer Leaflets and Aqueous Compartments of RBCs

Fresh human O-type RBCs were loaded with fluorescent aqueous dyes, either 6-carboxyfluorescein (CF; Molecular Probes, Eugene, OR) or ethidium bromide (Eth; Sigma Chemical Co.) or both, by mild hypotonic lysis (Ellens et al., 1989). The hypotonic solution contained either 5 mM CF or 1 mM Eth (or both) in 10 mM Tris-HCl, 0.5 mM EGTA, pH 7.5. Greater than 80% of the cells trapped the dyes. When required, these gray ghosts were "colabeled" with either the lipidic probes octadecylrhodamine B chloride (R18) or 1,1′-dihexadecyl-3,3,3′,3′-tetramethyl indocarbocyanine perchlorate (DiI; Molecular Probes). Colabeling is the labeling of RBCs with two fluorescent dyes, generally one aqueous, the other membrane. Intact RBCs were labeled with either R18 or DiI essentially as described (Morris et al., 1989).

Labeling Inner Leaflets of RBCs

The inner leaflets of RBCs were labeled with the fluorescent dyes FM1-43 and FM4-64 (Molecular Probes). FM1-43 has been the more widely used dye (Betz et al., 1992; Heuser et al., 1993). But because its emission overlaps that of both fluorescein and rhodamine, it was not suitable for colabeling of RBCs. We used FM4-64 when colabeling. Its emission in the far red (max. ex. 543 nm, max. em. 700 nm; Molecular Probes) does not interfere with the emission of CF, used to monitor continuity of aqueous compartments. Identical results of the dye spread from RBCs to HA-expressing cells were obtained with FM1-43 and FM4-64 under fusogenic conditions.

These dyes were introduced by lysing preswollen RBCs in hypotonic medium (10 mM Tris, 0.5 mM EGTA, pH 7.5) containing either 120–250 μg/ml of FM4-64 and 5 mM CF or 120–250 μg/ml of FM1-43, dissolved by intensive vortexing just before adding the medium to the suspension of RBCs. Then RBCs were incubated 2 min on ice, the osmolarity of the solution was restored by injection of 10× Hanks' medium, and RBCs were incubated at 37°C for 45 min. External FM and CF dyes were removed by three washes in large vols of PBS and the RBCs were stored on ice. The shape of RBCs was not noticeably affected by the FM dyes and the efficiency of CF entrapment was not diminished by FM4-64. The fluorescence from FM-labeled RBCs was faint compared with that of CF-labeled cells, but was easily detectable. These RBC membranes were irreversibly labeled by the FM dyes: staining persisted for more than 2 d at 4°C. Most, but not all, of the dye could be removed by repetitive washings with cold hypotonic buffer. In control experiments FM dyes were used to label RBCs externally, by a procedure analogous to that used with R18. The FM dyes were completely removed from the outer leaflets of the RBCs by three washes with PBS.

HA-WT and BHA-PI Cell Pretreatment and RBC Binding

As preparation for fusion experiments with erythrocytes, cells were grown to 40–60% confluency on 35-mm plastic dishes for about 24 h and washed twice with PBS. Cells were treated with 5 μg/ml trypsin (TPCK-treated; Sigma Chemical Co.) to cleave HA0 into its fusion-active, disulphide-linked HA1-HA2 form (or, as a control, with 5 μg/ml TLCK-chymotrypsin [Sigma Chemical Co.] to leave HA0 uncleaved) in the presence of 250 μg/ml neuraminidase (from *Clostridium perfringence*, type V; Sigma Chemical Co.) for 10 min at room temperature, essentially as described previously (Kemble et al., 1994). MEM containing 10% FCS was added to inhibit the protease, and the cells were washed three times with PBS. These cells were incubated with a 1-ml suspension of erythrocytes (0.05% hematocrit) for 15 min at room temperature with occasional gentle rocking; the unbound RBCs were removed by rinsing three times with PBS, and the cells remaining were used for experiments within 1 h. Fusion was triggered at room temperature by replacing PBS with an isotonic pH = 4.9 solution (100 mM NaCl, 2.5 mM $CaCl_2$, and 20 mM succinate), for 2 min. The acidic solution was then substituted by a pH = 7.4 solution (110 mM NaCl, 1.5 mM KCl, 2 mM $MgCl_2$, 2 mM $CaCl_2$, 1 mg/ml glucose, and 20 mM Hepes). When measuring transfer of Eth, 0.1 mg/ml of DNA (from salmon testes, Sigma Chemical Co.) was included in the pH = 7.4 solution to bind any Eth that might leak into the external solution. When required, osmotic swelling of RBCs was achieved by replacing the media with 72 mOsm solutions at neutral pH for 30 s, followed by reintroducing isotonic media.

Cell to Planar Lipid Bilayer Membrane Fusion

For cell–bilayer fusion experiments, cells were treated essentially as reported (Melikyan et al., 1993*a*). HA-WT and BHA-PI cells were grown on 100-mm dishes to ~90% confluency, washed twice with PBS, and lifted from the dish by incubation with PBS containing 0.5 mg/ml trypsin, 0.5 mg/ml EDTA for 2 min at 37°C. Trypsin was quenched by adding an excess of MEM with 10% FCS. Cells were collected from the dish, pelleted, and resuspended in PBS containing 0.25 mg/ml neuraminidase. After a 6-min incubation at 37°C, cells were washed twice with PBS and resuspended at ~10^7 cells/ml in a small vol of PBS and stored on ice for up to 4 h.

Cells with uncleaved HA0 were obtained by lifting them from dishes after incubation for 6 min at 37°C in trypsin-free PBS containing 0.5 mg/ml EDTA/0.5 mg/ml EGTA, 50 μg/ml chymotrypsin (TLCK-treated), and 20 μg/ml soybean trypsin inhibitor (STI; Sigma Chemical Co.). The chymotrypsin was then quenched by adding an excess of MEM with 10% FCS. Cells were pelleted, resuspended in PBS with 250 μg/ml neuraminidase, 40 μg/ml STI, and then incubated 6 min at 37°C. After washing twice with PBS, cells were resuspended in PBS with 20 μg/ml STI and stored on ice.

Solvent-free horizontal bilayer membranes were formed in a chamber mounted on a stage of an inverted microscope (Diaphot; Nikon Inc., Instrument Group, Melville, NY) as described (Melikyan et al., 1993*a*). The membranes were formed within a 160-μm hole in a 50-μm-thick black Teflon partition bathed by 140 mM NaCl, 2.5 mM KCl, 5 mM $MgCl_2$, 2 mM $CaCl_2$, and 1 mM Pipes, pH 6.5, and maintained at 37°C. Membranes were formed from dioleoylphosphatidylcholine (DOPC; Avanti Polar Lipids, Pelham, AL), dioleoylphosphatidylethanolamine (DOPE; Avanti), and lissamine rhodamine B sulfonyl labeled DOPE (rhoPE; Avanti Polar Lipids) (DOPC/DOPE/rhoPE, 5:2:1 wt/wt) dissolved in squalene (Aldrich Chemical Co., Milwaukee, WI) that was purified over activated alumina. Including 4 M % of the ganglioside G_{D1a} in the membrane did not significantly affect fusion kinetics, presumably because X:31 HA preferentially binds to α2-6–linked sialates (Rogers and Paulson, 1983), whereas gangliosides predominantly have α2-3 linkages. Experiments were initiated by injecting a small volume (5–10 μl) of a concentrated cell suspension over the horizontal bilayer. Approximately 15–25 cells sedimented onto the membrane. Most of the other cells landed on the large Teflon partition. After cells adhered to the planar bilayer for 4–5 min, fusion was triggered by injecting 25 μl of a concentrated isotonic succinate pH = 4.9 solution around the cells.

Electrical Measurements

Planar lipid bilayers were voltage clamped and the electrical admittance was obtained as a function of time (Melikyan et al., 1993*a*,*b*). In brief, a sinewave voltage, of frequency f = 1 kHz, superimposed on a constant holding potential was generated by computer (486DX2/66, VTECH Computers, Lake Zurich, IL) and applied to the membrane. The admittance components in-phase, Y_0, and out-of-phase, Y_{90}, with respect to the applied sinewave, as well as the direct current (dc) conductance, Y_{dc}, were obtained on line and saved to a hard disk. These three measures yielded the three parameters used to model fusion of HA-WT cells to planar membranes: the conductance of fusion pores, g_p, in series with the parallel combination of cell conductance, G_c, and cell capacitance, C_c. The capacitance of the planar membrane was electronically compensated and its conductance was initially small and could be ignored. After acidification, the bilayer conductance would increase over time, but because a fusion pore had usually fully enlarged before such increases, g_p could be unambiguously calculated for HA-WT cells.

However, for BHA-PI cells, admittances changed slowly. These changes could, in principle, result from current through two separate routes. One aqueous pathway would connect the cell free trans (bottom) solution of the bilayer to the interior of the cell; the other would connect the top and bottom solutions directly through the planar bilayer. We refer to the conductances from the cell interior to the trans side of the bilayer as "hemifusion diaphragm–associated conductances," g_{hd}, because, as we will show, these currents occurred after hemifusion and flowed through hemifusion diaphragms that connected cell and planar membranes. Increases in Y_0 were the earliest resolved electrical activities. But not until $Y_0 - Y_{dc} > 0$, could we be absolutely certain that g_{hd} had increased. (If current only flowed directly through the bilayer, $Y_0 = Y_{dc}$.) Because the conductance and capacitance of the planar bilayer could vary on the time scale of changes in g_{hd}, there were too many unknown parameters for g_{hd} to be calculated definitively. But when g_{hd} was not too large (<30 nS) it could be bounded: Y_0 set an upper bound and $Y_0 - Y_{dc}$ provided a lower bound for g_{hd} (Lindau and Neher, 1988; Spruce et al., 1989; Melikyan et al., 1993*a*). If G_c were zero, $Y_0 - Y_{dc}$ would equal g_{hd}, even if current flowed directly through the bilayer as well as through the hemifusion diaphragm. In practice, G_c was not zero and this caused $Y_0 - Y_{dc}$ to underestimate g_{hd}, and we could not measure g_{hd} until it was on the order of 1 nS. If $G_c = 0$, our resolution would be about 0.3 nS at 1 ms. We verified our assignment for the route of current pathways by checking that hemifusion did not occur when increases in electrical activity were due to increases in bilayer conductance: when the electrical activity was clearly due to conductance pathways within the planar bilayer proper, and not due to g_{hd}, spread of rhoPE was not observed (see Video Microscopy).

Video Microscopy

Transfer of fluorescent dyes from RBCs or planar membranes to transfected cells was viewed with an inverted microscope (Diaphot; Nikon Inc., Instrument Group) using epifluorescence through either a long working distance objective (MPlan 20×/0.4 NA, ELWD; Nikon Inc., Instrument Group) or a phase-contrast objective (20×/0.4 NA, Nikon Inc., Instrument Group). The light from the objective was passed through a projection lens at a magnification of 2.5, focused onto the faceplate of a video camera (SIT 66; Dage-MTI, Inc., Michigan City, IN), set at maximum gain, and recorded on a VHS format VTR (model SLV-393; Sony Communication Co., Parsippany, NJ) for later analysis. When using Eth, rhoPE, R18, DiI, or FM4-64 as the fluorescent dye, a rhodamine filter cube was selected (G2A; Nikon, ex 510–560 nm, dichroic mirror 580 nm, em >590 nm). CF and FM1-43 fluorescence was monitored with a fluorescein filter cube (B, Nikon, ex 420–485 nm, dichroic mirror 510 nm, em 520–560 nm). There was no detectable fluorescence from rhoPE and R18 when using the fluorescein cube and no measured fluorescence from CF when using the rhodamine cube, allowing two dyes (e.g., CF and R18) to be monitored in the same experiment by repetitive switching of cubes. To obtain hard copies of pictures, selected frames of video tape were transferred to an optical disk recorder (TQ3038F; Panasonic, Secaucus, NJ) with time-base correction (Novasync 2F; Nova Systems, Inc., Canton, CT). These images were digitized at 512 × 480 resolution (series 151; Imaging Technology Inc., Bedford, MA), the contrast adjusted, and printed (Linotype 530, Hell AG, Eshborn, Germany).

In cell to bilayer experiments, membrane dye mixing was monitored by placing a high concentration (12 mol%) of rhoPE in the planar bilayer. The fluorescence of this high concentration of rhoPE was significantly, but not completely, self-quenched (MacDonald, 1990). The fluorescence of the dye in the bulk squalene comprising the torus (technically the Gibbs-Plateau border) surrounding the planar membrane was particularly bright. Therefore, the field diaphragm for the epifluorescence pathway was barely opened to minimize the diameter of the light beam (to ~120 μm) so that the torus was not directly excited. Electrical and fluorescence signals were synchronized by sending a computer-generated TTL pulse to a date/time generator (model 401; Vista Electronics, Mesa, CA), marking time = 0 on both the video tape and on the computer-recorded electrical signals. Time = 0 was routinely set when the acidic solution was injected around the cells. When the cell membrane and lipid bilayer established continuity, the rhoPE diffused into the cell, diluted, and relieved quenching, yielding increases in fluorescence. The onset of dequenching was determined visually by playing the video tape in frame-by-frame mode. With BHA-PI cells, the onset of increases in fluorescence significantly preceded any electrical signals, alleviating the need for computer-aided image analysis.

Results

Lipid Dye, But Not Aqueous Dye, Spreads between RBCs and BHA-PI Cells under Fusogenic Conditions

We colabeled the RBCs by trapping the dye CF into their aqueous interiors and then incorporating the lipid dye R18 into their cell membranes. The colabeled RBCs transferred R18 to both HA-WT (Fig. 1 *A*) and BHA-PI (Fig. 1 *C*) cells under fusogenic conditions. But only the HA-WT cells took up CF (Fig. 1, *B* and *D*), consistent with previous observations (Kemble et al., 1994). Both the wild-type (wt) HA0 (Fig. 1, *E* and *F*) and the GPI-linked HA0 of BHA-PI cells (Fig. 1, *G* and *H*) had to be cleaved into HA1-HA2 subunits for dye transfer to occur. Labeling RBCs with the fluorescent lipid probe DiI in place of R18 led to the same results (data not shown). Virtually all BHA-PI cells with bound RBCs became labeled with the lipid probes, but no cells became labeled with the aqueous content probe.

We attempted to improve the ability to detect small and/or transient fusion pores between RBCs and BHA-PI cells, if they occur, by loading RBCs with 1 mM Eth (mol wt 394). Eth intercalates within DNA, leading to both a major increase in fluorescence quantum yield (LePecq and Paoletti, 1967) and irreversible accumulation in the cell nucleus. Both these factors would aid detection of aqueous dye transfer. We established that Eth was indeed a better detector of aqueous continuity than CF by colabeling RBCs with 5 mM CF as well as Eth: some HA-WT cells stained by Eth were not stained by CF, but all cells labeled by CF were also labeled by Eth. Although cells labeled by both dyes were more brightly stained by CF (Fig. 2, *A* vs. *B*),

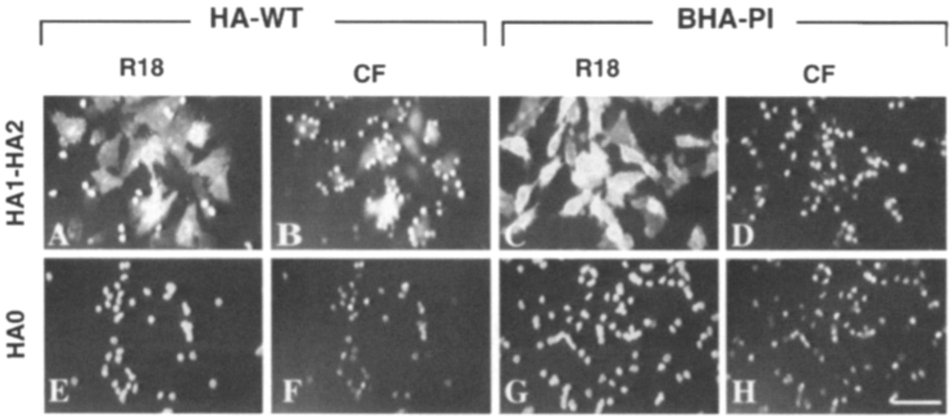

Figure 1. Aqueous and lipidic dye mixing with HA-WT and BHA-PI cells. RBCs colabeled with CF and R18 were bound to HA-WT (*A, B, E, F*) or BHA-PI (*C, D, G, H*) cells and fusion was triggered by a 2-min exposure to pH = 4.9. After a 30-min incubation at neutral pH buffer, dye transfers from RBCs to HA-expressing cells were microscopically examined. While wt-HA caused transfer of both R18 (*A*) and CF (*B*), GPI-HA demonstrated only R18 mixing activity (*C*). CF remained within RBCs for up to 1 h (*D*). (*E–H*) demonstrate the absence of dye mixing in control experiments with HA-WT (*E* and *F*) and BHA-PI (*G* and *H*) cells expressing uncleaved HA0. Neither CF (*F* and *H*) nor R18 (*E* and *G*) spread was observed for those cells under fusogenic conditions. To examine the fluorescence of CF, the intensity of the excitation beam was attenuated to 12.5% with a neutral density filter to avoid overloading the video camera. Bar, 50 μm.

cells stained by Eth were visible. Importantly, after a 2-min acidification followed by reneutralization, virtually none of the BHA-PI cells were stained by Eth (Fig. 2 *F*) for up to 45 min. Thus, HA-WT cells exhibit aqueous continuity with RBCs under fusogenic conditions, but BHA-PI cells do not. Without the low pH pulse, or without cleaving HA0 fusion did not occur: neither CF nor Eth entered HA-WT cells (Fig. 2, *C* and *D*).

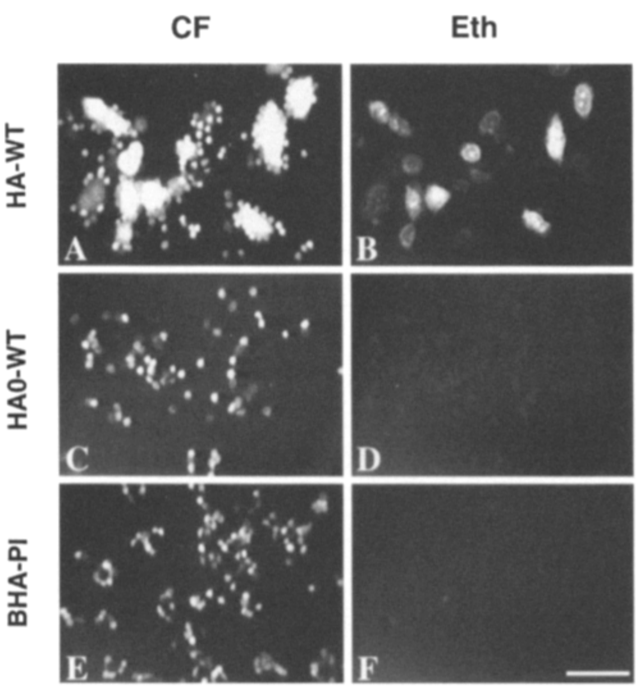

Figure 2. Transfer of the aqueous dyes CF and Eth from RBCs into HA-WT (*A–D*) and BHA-PI (*E* and *F*) cells. Free Eth is weakly fluorescent (*D* and *F*); colabeling with CF allowed the RBCs to be visualized (*A, C,* and *E*). Fusion was triggered by a 2-min exposure to pH = 4.9 (see legend to Fig. 1 for details). Cleaved HA1-HA2 induced effective CF (*A*) and Eth (*B*) transfer into HA-WT cells. As expected, Eth accumulated within cells, making them clearly visible. In contrast, neither CF (*E*) nor Eth (*F*) usually transferred into BHA-PI cells. However, ~1% of the BHA-PI cells did become faintly labeled with Eth (not shown). This likely is due to the fact that at low pH HA increases permeabilities of membranes. *C* and *D* show that neither dye moved into uncleaved HA0-expressing HA-WT cells. When the GPI-HA0 of BHA-PI cells were not cleaved absolutely no dye transfer was observed (data not shown). Bar, 50 μm.

Inner Leaflets of RBC Membranes Become Continuous with HA-WT Membranes But Not with BHA-PI Cell Membranes at Low pH

Transfer of R18 established that the outer bilayer leaflets of HA-WT and BHA-PI cells became continuous with the outer leaflets of RBCs after triggering fusion. We explored mixing between inner, cytosolic leaflets by labeling the inner leaflets of RBCs with FM1-43 or FM4-64 (see Materials and Methods). These doubly charged, membrane-impermeant, cationic dyes fluoresce well when inserted in membranes, but fluoresce poorly in aqueous solution (Betz et al., 1992; Heuser et al., 1993). Additionally RBCs were loaded with CF so that the relation between aqueous and inner leaflet continuity could be assessed. Whenever HA-WT cells became labeled with CF (Fig. 3 *A*), they were stained by FM4-64 (Fig. 3 *B*) within a few minutes after acidification. In fact, the staining was much faster with FM4-64. But some cells stained by FM4-64 had not become detectably labeled by CF (*arrows*, Fig. 3, *B* vs. *A*), despite the fact that CF provided the brighter fluorescence for cells stained by both dyes. Thus, FM4-64 did not transfer via the aqueous lumen of the fusion pore because it is somewhat larger and much more hydrophobic than CF, the latter causing a small aqueous concentration of FM4-64 within the RBCs. FM4-64, therefore, moves along the inner walls of the fusion pore and is a more sensitive reporter of small pores than are aqueous dyes. The fact that generally neither FM4-64 (Fig. 3 *F*) nor CF (Fig. 3 *E*) transferred from RBCs to BHA-PI cells under fusogenic conditions is strong evidence for hemifusion. As expected, with uncleaved wt HA0, neither dye transferred out of the RBCs (Fig. 3, *C* and *D*). Similarly, uncleaved GPI-HA0

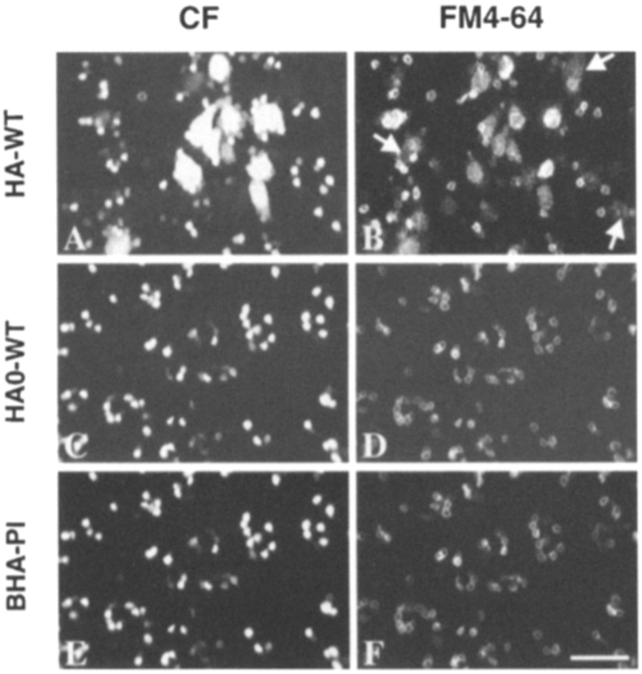

Figure 3. Assessing the continuity of the inner leaflets of RBCs with those of HA-WT (*A–D*) or BHA-PI (*E* and *F*) cell membranes. RBCs were colabeled with CF (*A*, *C*, and *E*) and FM4-64 (*B*, *D*, and *F*). FM4-64 was selectively incorporated into the inner leaflet of the RBC membranes. Under fusogenic conditions both CF (*A*) and FM4-64 (*B*) moved from RBCs into HA-WT cells, but not into BHA-PI cells (*E* and *F*, respectively). Notice that more cells were stained by FM4-64 than by CF (arrows on *B* vs. *A*). The cytosolic concentration of FM4-64 was lower than CF as demonstrated by the difficulty of removing FM4-64 from inner leaflets of RBCs by hypotonic lysis (see Materials and Methods), whereas CF was easily removed. Because FM4-64 is larger than the water-soluble CF, the faster kinetics and higher percentage of cells stained by FM4-64 implies it transferred via movement within the inner leaflets and not through the aqueous pathway of fusion pores. Dye did not transfer in HA0 control experiments as shown for HA-WT cells (*C*, CF; *D*, FM4-64). Bar, 50 μm.

did not produce any dye spread into BHA-PI cells (data not shown). Thus, the outer but not the inner leaflets of BHA-PI cells and RBCs become continuous under fusogenic conditions, exactly what one would expect in a state of hemifusion.

A small percentage (5–8%) of the BHA-PI cells became labeled by FM4-64 ~20 min after reneutralization (which followed the standard 2-min exposure to low pH). Unlike FM4-64, R18 quickly spread to all bound BHA-PI cells, within the 2-min low pH incubation. It is conceivable that FM4-64 itself tends to destabilize the hemifusion diaphragm: CF did not transfer to BHA-PI cells when RBCs were labeled with CF alone, but ≈2% of the BHA-PI cells were stained by CF when RBCs were colabeled with FM4-64. Taken together, the data shows that wt-HA induces complete fusion whereas GPI-HA mediates hemifusion.

Osmotic Swelling of Hemifused Cells Induces Full Fusion

We investigated the area of membrane shared by hemifused RBCs and BHA-PI cells. After R18 redistributed from RBCs to BHA-PI cells (Fig. 4 *A*), the RBCs were osmotically swollen and transfer of CF (Fig. 4 *C*) into the BHA-PI cells (Fig. 4 *D*) was monitored. If hemifusion was transient or its area small, with dimensions on the order of molecular sizes, the osmotically lysed RBCs would release virtually all dye to the external medium. In contrast, if there was an extended hemifusion diaphragm that was long-lasting, some lysis would occur in the diaphragm forming a pore that allows transfer of dye to the hemifused BHA-PI cells. If all RBCs were lysed, the fraction of BHA-PI cells that became labeled by CF after osmotic swelling would provide an estimate of the areas of the diaphragms relative to the areas of RBC membranes that were not part of the diaphragm, assuming comparable stability against osmotic stress in the two regions. A brief application of hypotonic solution caused swelling and exten-

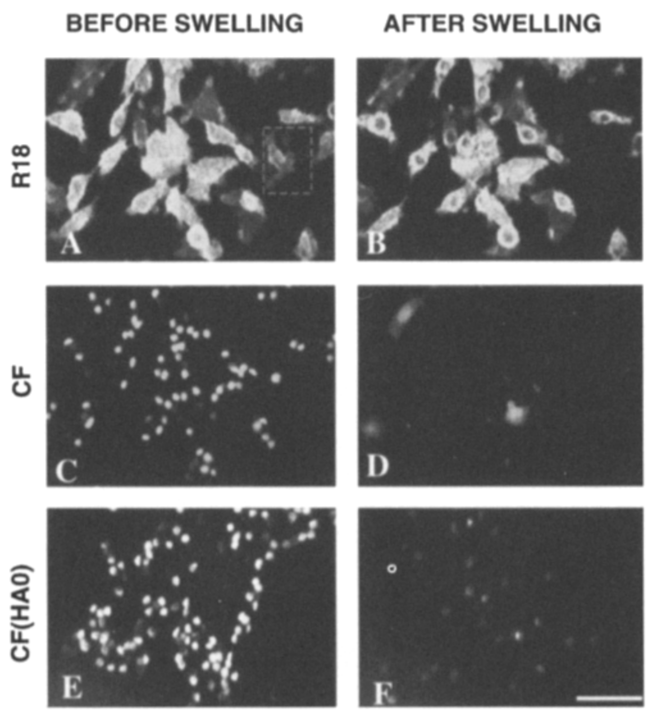

Figure 4. Osmotic swelling induces aqueous dye transfer from RBCs to BHA-PI cells. RBCs colabeled with CF (*C–F*) and R18 (*A* and *B*) were bound to BHA-PI cells, acidified to pH = 4.9 for 2 min and returned to neutral pH for 20 min. R18 completely redistributed to the BHA-PI cells (*A*) whereas CF remained within the RBCs (*C*). The isotonic solution was replaced by a hypotonic one (72 mOsm). The RBCs swelled and lysed; virtually all RBCs released CF to either the external solution or into adhered BHA-PI cells. After 30 s cells were returned back to isotonic solution, removing a high fluorescent background. *B* and *D* show the same cells, as in *A* and *C*, after this hypotonic treatment. The pattern of R18 fluorescence was virtually unaffected (*B* vs. *A*). A few RBC and BHA-PI cells (*A*, *dotted box*) disappeared (*B*) due to mechanical displacements upon changing the solutions. CF has transferred into some BHA-PI cells after swelling, seen as three fluorescent cells (*D*). The same osmotic swelling protocol with HA0-expressing BHA-PI cells (shown for CF, *E*) led to extensive lysis without transfer of either R18 or CF from RBCs (*F*). Bar, 50 μm.

sive lysis of RBCs, releasing CF into the external solution. Using a 72-mOsm external solution to insure that most (>90%) RBCs released dye, ~10–15% of the BHA-PI cells that bound RBCs became fluorescent (Fig. 4, *D* vs. *C*). That is, we induced full fusion for these 10–15% of the BHA-PI cells. As typically 3–5 RBCs were bound to a BHA-PI cell, we estimate that each diaphragm had an area on the order of several percent (10–15% divided by 3–5) of the RBC membrane area. A precise area could not be calculated as different osmotic pressures were probably required to destabilize hemifused and nonhemifused membranes.

The spread of R18 was complete before osmotic swelling; the swelling did not affect the R18 staining pattern of the BHA-PI cells (Fig. 4, *B* vs. *A*). Swelling did, however, result in redistribution of FM4-64 from RBCs to BHA-PI cells (data not shown). If pH was lowered but GPI-HA0 not cleaved (Fig. 4 *E*), or the HA0 cleaved but pH not lowered (data not shown), the same lysis protocol caused all the CF to be released into the external medium (Fig. 4 *F*) (<0.1% of the BHA-PI–expressing cells expressing GPI-HA0 acquired CF).

Fusion Pores Form Before Observed Spread of Lipid When HA-WT Cells Fuse to Planar Membranes

To detect the formation of fusion pores electrically, cells were settled onto a horizontal planar bilayer and the pH of the top solution was lowered to and maintained at 4.9. The electrical responses with HA-WT and BHA-PI cells were distinctly different: within seconds of lowering pH, fusion pores typically formed for HA-WT cells (Fig. 5, upper electrical trace), but did not form for BHA-PI cells (lower trace). For HA-WT cells, pores repetitively opened and closed, a phenomenon referred to as flickering. Flickering is a hallmark characteristic of fusion pores connecting HA-expressing cells to planar membranes (Melikyan et al., 1993*b*, 1995*a*,*b*). (It has been observed for the three strains of HA tested.) A pore then securely opened and exhibited semistable conductances, in the range of 2–20 nS roughly corresponding to diameters of 5–25 nm, before fully enlarging with a stepwise conductance increase to about 1 μS, diameter ≈1 μm (Fig. 5, marked by asterisk in upper electrical trace).

Membrane continuity was assessed by including a self-quenching concentration of the fluorescent lipid probe rhoPE (12 M %) in the planar bilayer. Spread of dye into HA-WT cells was always observed after the appearance of pores, never before. In fact, usually a pore fully enlarged to ~1 μS before any spread of dye was observed. When this occurred, the first change in fluorescence observed was a quickly enlarging dark spot on the bilayer at the site of the fusing cell (Fig. 5 *C*). This complete removal of fluorescent lipid over an extended area was undoubtedly caused by the tension of the planar bilayer pulling membrane of the fused cell through the large fusion pore, thereby displacing fluorescent lipid by the flow of cell lipids and possibly cell proteins. Some tens of seconds later, after the rhoPE diffused into the dye-depleted area, the cell started to become fluorescent (*D*). With time, the cell would become quite bright (not shown). At neutral pH pores did not form and cells did not become fluorescent for up to 20 min.

Membrane Dye Spreads without Fusion Pore Formation for BHA-PI Cells

In distinct contrast to HA-WT, rhoPE spread from planar membranes to BHA-PI cells after acidification (Fig. 5, marked by arrow in *G* and labeled *G* in lower electrical trace) but before any electrical activity (note the shorter time scale for HA-WT cells than for BHA-PI cells in the electrical trace). This unequivocally demonstrates that lipid continuity was established between BHA-PI cells and planar membranes before any connections between cytoplasm and cell-free, bottom, aqueous compartments. While fusion pores characteristic of wild type never formed, at relatively long times after acidification, gradual and irreversible increases in conductance of the hemifused diaphragm, g_{hd}, occurred (Fig. 5, lower electrical trace). With time, the first cell that hemifused became increasingly fluorescent and more cells became labeled (Fig. 5 *H*).

After hemifusion occurred, the cytosol of a cell would still be separated from the bottom solution bathing the planar membrane by a shared single bilayer. One leaflet would be contributed by the cell, the other by the planar membrane. This bilayer would be asymmetric and under stress because of the tension of the planar membrane, possibly accounting for the occurrence of g_{hd}. To test this idea, we included cholesterol (30 M %) in the bilayer because it is known to stabilize membranes and reduce nonspecific leaks in bilayers (Papahadjopoulos et al., 1971). As expected, this led to reduced g_{hd}. Spread of rhoPE was still observed (data not shown). This is consistent with a g_{hd} caused by nonspecific conductance increases rather than by fusion pores. Control experiments with HA-WT cells showed that including cholesterol in the planar membrane did not appreciably affect the kinetics of formation of fusion pores.

The kinetics of fusion pore formation and onset of hemifusion were characterized by waiting time distributions. The times from acidification until rhoPE labeling of BHA-PI cells (Fig. 6, *open diamonds*) were distributed over appreciably shorter times than for the onset of any electrical activity (*closed triangles*). The earliest electrical activity was too small to allow g_{hd} to be distinguished from bilayer conductance (see Materials and Methods). But when the currents became large enough to allow differentiations to be made, generally the electrical response was due to increases in g_{hd}. Therefore the onset of electrical activity (Fig. 6, *closed triangles*) preceded unambiguous increases in g_{hd} (*closed squares*), both occurring after lipid dye redistribution. The distribution of times from acidification until the appearance of the first flickering pore was also generated for HA-WT cell experiments (Fig. 6, *closed circles*). In agreement with the representative examples shown (Figs. 5 and 7), the distributions demonstrate that flickering pores formed for HA-WT cells considerably more quickly than any process observed with BHA-PI cells.

If HA0 was not intentionally cleaved, fusion and hemifusion did not occur over the time courses effects were observed with cleavage-activated HA. However, occasionally increases in g_{hd} occurred for both HA-WT and BHA-PI cells at times an order of magnitude greater than effects were observed with cleaved wt-HA and cleaved GPI-HA. It is likely a low level of cleaved HA was present in these experiments.

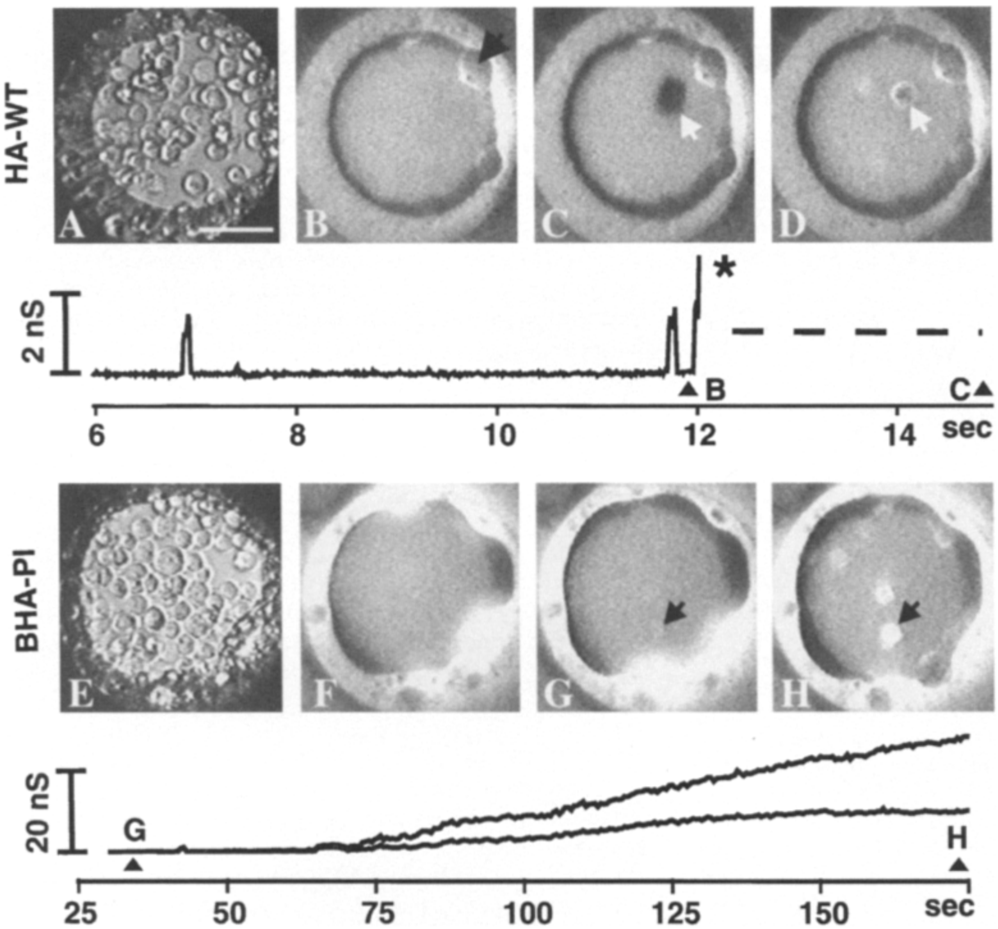

Figure 5. Simultaneous monitoring of lipid mixing and conductance increases between HA-expressing cells and rhoPE-containing planar bilayers. (*Top*) Simultaneous measurements of rhoPE fluorescence dequenching and fusion pore conductance for HA-WT fusion to planar bilayer. After fusion was triggered by acidification (time = 0) of the cell-containing compartment, fusion pores twice opened transiently (flickers), then a pore opened irreversibly and enlarged quickly (asterisk on conductance trace) to conductances on the order of 1 μS, which corresponds to a pore diameter of ~1 μm. (*A*) Bright-field image of a 160-μm horizontal planar membrane with multiple adhered cells. The torus (a semitransparent ring on the picture) consists of a lipid/squalene mixture and provides a connection between the planar bilayer (center) and the supporting teflon partition. Cells settled onto the partition, torus, and bilayer. Electrical signals derive only from the solvent-free bilayer. (*B*) After two flickers, cells have not yet become fluorescent (*arrowhead B* on the conductance trace). An irrelevant fluorescent lipid bubble, below the planar membrane, appeared (*black arrowhead*). (*C*) A few seconds after a pore has fully enlarged (*arrowhead C* in conductance trace) a large dark area (*arrow,* shown at its maximum area) appeared. The dashed horizontal line to the right of the conductance trace indicates the time from the initial darkening until growth to maximum area (which exceeded the fusing cell diameter, *C*). (*D*) rhoPE dequenching pattern (*arrow*) shown 44 s after acidification. The circumference of the fused cell appeared as a bright ring due to dequenching of rhoPE upon diffusing into the cell. (*Bottom*) rhoPE mixing and g_{hd} of BHA-PI cells hemifused to planar bilayers. In contrast to wild-type HA, after acidification a fluorescence signal was detected before electrical activity (*G*, marked as *arrowhead G* in electrical trace). g_{hd} typically appeared after a long delay and increased slowly. g_{hd} was bounded between the upper (Y_0) and lower ($Y_0 - Y_{dc}$) traces (see Materials and Methods). Conductance increases occurred over much slower time scales (shown in conductance traces) for BHA-PI than for HA-WT cells. (*E*) Bright-field image of BHA-PI cells adhered to planar bilayer. (*F*) Fluorescence pattern before fusion was triggered. (*G*) Onset of rhoPE dequenching (*arrow*) 35 s after acidification. (*H*) Further spread of rhoPE from the bilayer to a cell, manifested as a slow increase in fluorescence intensity and appearance of other cells that have established membrane continuity with the planar bilayer (173 s after lowering pH, *arrowhead H* on conductance trace). Bar, 50 μm.

Movement of Eth Verifies Electrical Measurements

We confirmed that electrical detection of fusion pores was indeed due to aqueous connections between cell interiors and bottom solutions by examining the spread of Eth. Eth placed in the bottom solution fluoresced slightly, giving rise to a small background fluorescence (Fig. 7, *B* and *E*). Eth passed through fully enlarged μS fusion pores, within a few seconds of the enlargement, and brightly stained the fused HA-WT cell (Fig. 7 *C*, *arrow* and upper electrical trace). In contrast, much less Eth entered BHA-PI cells through hemifusion diaphragms with g_{hd} on the order of several nS. Even at very late times after acidification and well after g_{hd} appeared (Fig. 7, note again shorter time scales for HA-WT, upper trace, than for BHA-PI cells, lower trace), there was only a modest fluorescence increase of a hemifused BHA-PI cell (stained cell marked by arrow in Fig. 7 *F*, marked *F* in electrical trace). When the values of g_{hd} were small, BHA-PI cells never became very bright. Sometimes g_{hd} became large, on the order of hundreds of nS. When this happened, a BHA-PI cell became highly stained by Eth (not shown).

Area of the Hemifused Diaphragm between BHA-PI Cells and Planar Bilayers Can Become Large

Osmotic swelling experiments (Fig. 4) indicated that the bilayer diaphragm connecting hemifused BHA-PI cells and RBCs was extended, not local. We conducted fluorescence and electrical experiments to determine whether the hemi-

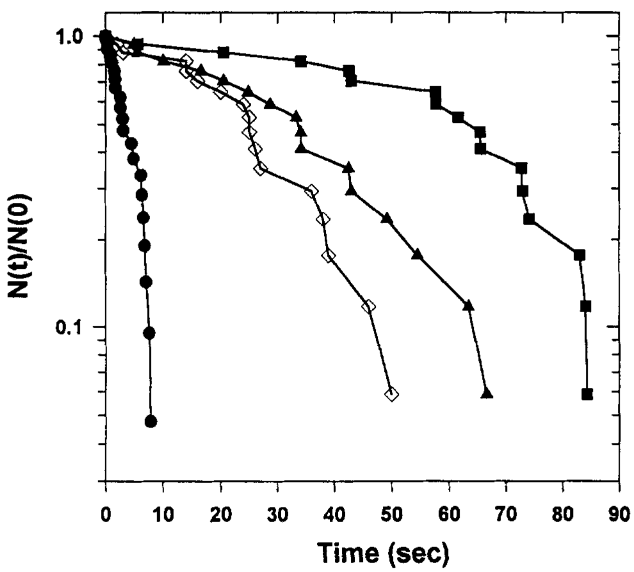

Figure 6. Kinetics for conductance and fluorescence signals under fusion conditions. Kinetics were obtained by producing waiting time distributions from single events. The waiting times are presented as survivor distributions; the fraction of events, N(t)/N(0), that take time >t. The distribution for the first fusion pore to form (*filled circles*) between HA-WT cells and planar bilayers was relatively fast, without appreciable lag and roughly exponential. In contrast, the onsets of g_{hd} increases for BHA-PI cells (*filled squares*) were distributed over longer times, had pronounced lags, and a complex shape. Membrane dye spread was always observed before increases in g_{hd}: the waiting times for a fluorescence dequenching signal (*open diamonds*) were much shorter than for onset of any electrical signals (*closed triangles*, see Materials and Methods) which in turn were shorter than for onset of g_{hd} increases (*filled squares*).

fused diaphragm between BHA-PI cells and planar membranes was also large. When cells were merely adhered to the planar membrane (Fig. 8 *A*), the fluorescence brightness of the rhoPE-containing bilayer was uniform (Fig. 8 *B*). After acidification, BHA-PI cells that hemifused were identified by staining of cells with rhoPE (Fig. 5). For these cells, the initial fluorescence changes exhibited two distinct patterns. For about two-thirds of the hemifusion events, dequenching of rhoPE was detected as an increase in BHA-PI cell brightness. For the other one-third of the cases, an extended area became somewhat darker at the location of a cell that would subsequently become fluorescently labeled (Fig. 8 *C*, *arrow*). The darkening is probably a direct consequence of hemifusion: contacting monolayer leaflets are cleared from the hemifusion diaphragm which results in replacement of labeled lipid probe within the contacting leaflet of the planar membrane by unlabeled lipids of the inner leaflet of the hemifused cell membrane. This dark area was usually more or less circular, but could assume the irregular shape of the hemifused cell as in Fig. 8 *C*. The brightness profile of this area evolved into a "donut" shape within ~10 s, bright on the circumference and dark in the middle (Fig. 8 *D*). This is expected for an extended diaphragm: dye from the bilayer would initially diffuse into the circumference of the newly created diaphragm. The concentration of probe would be lower in the rim than in the bilayer proper, the probe fluorescence would not be quenched there, and a toroid of brightness would result. The entire area over which fluorescence was changing and the cell itself then slowly became fluorescently labeled (Fig. 8 *E*). By this point, the affected area was always circular. The change in shape in Fig. 8, from irregular to circular, would be explained by the uniform pull of the tension of the bilayer on the hemifused diaphragm. For the two-thirds of the cases where only increases in cell brightness were observed, either the hemifusion diaphragm never enlarged or it enlarged slowly. In the latter case, the bright cell membrane would have obscured the slowly enlarging dark diaphragm. In any case, brightness changes occurring over an extended area is evidence of a large hemifused diaphragm, as is the time course and geometric pattern of the changes. None of these changes would be expected if membrane continuity occurred only over a small restricted region.

The area of the hemifusion diaphragm was also evaluated electrically. When pores fully enlarged, the capacitances of fused cells were fully revealed and corresponded to cell capacitances determined in whole-cell patch clamp measurements (Melikyan et al., 1993*a*). After full pore enlargement, the capacitances of HA-WT cells were measured to be 17.3 ± 0.9 pF, n = 95. After hemifusion of a BHA-PI cell, the cell membrane was distributed between the hemifusion diaphragm and the region not incorporated into the diaphragm. The capacitances (areas) of the regions of hemifused cells that were not incorporated into the hemifusion diaphragms were revealed for BHA-PI cells when g_{hd} enlarged quickly, as occurred in a fraction of the experiments. These capacitances, 8.0 ± 0.8 pF, n = 54, were much lower than the capacitances of HA-WT cells. Both lines were derived from the same initial CHO cell line (Kemble et al., 1993), and their size distributions were indistinguishable as determined by light scattering using a cell sorter (data not shown). The differences in measured capacitances indicate that appreciable fractions of BHA-PI cell membranes were incorporated into hemifusion diaphragms. If all the assumptions used to compare the capacitances are correct, these measurements show that one-half of the BHA-PI cell membrane became incorporated into the diaphragm: the hemifusion diaphragm and the nonhemifused region of the cell had approximately the same areas. Thus, electrical measurements reinforce the observation of fluorescence: the hemifusion diaphragm is extended.

Discussion

Hemifusion has long been conjectured as an intermediate of fusion (Palade, 1975; Pinto da Silva and Nogueira, 1977; Kalderon and Gilula, 1979; Chernomordik et al., 1987; Lucy and Ahkong, 1986; Nanavati et al., 1992). There is abundant evidence that hemifusion can occur in model lipid membrane systems (Neher, 1974; Ellens et al., 1985; Leventis et al., 1986; Chernomordik et al., 1987, 1995; Helm et al., 1992) and in artificially induced fusion between biological membranes (Stenger and Hui, 1986; Song et al., 1991; Ahkong et al., 1987). However, there has been scant experimental support that protein-mediated biological fu-

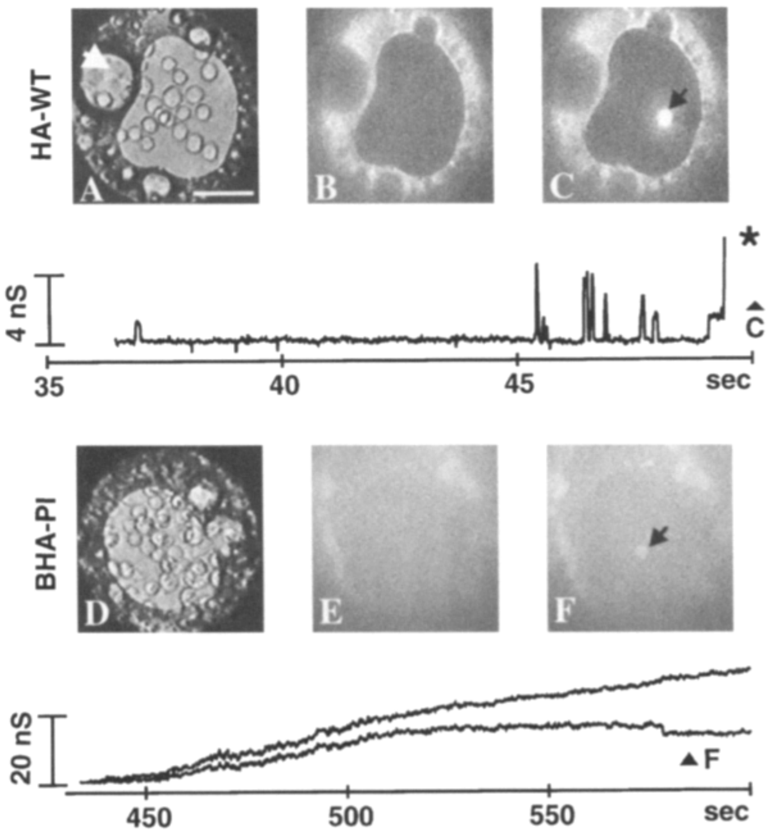

Figure 7. Simultaneous monitoring of aqueous dye mixing and conductance increases between HA-expressing cells and planar bilayers. (*Top*) Temporal correlation between fusion pore evolution and Eth entry into cytosol of HA-WT from the cell-free (trans) side of planar bilayers. The typical pattern of fusion pore evolution occurred: pore flickerings followed by an instantaneous enlargement (asterisk on electrical trace) to the diameter range of μm. (*A*) A bright field picture of a planar bilayer with HA-WT cells adhered to it (*white arrowhead* indicates an inconsequential water bubble trapped in the torus upon bilayer formation). (*B*) Background fluorescence with 0.2 mM Eth in the trans solution bathing the bilayer. (*C*) Fast increase of fluorescence (*arrow*) due to Eth easily permeating the large fusion pore and intercalating within nucleic acids of the nucleus (*arrowhead C* on conductance trace). (*Bottom*) Monitoring the aqueous continuity between the cytosol of BHA-PI cells and the cell-free compartment of the planar bilayer upon increases in g_{hd}. Bounded between upper (Y_0) and lower ($Y_0 - Y_{dc}$) traces, g_{hd} developed slowly, starting 430 s after acidification. (*D*) Bright-field picture of BHA-PI cells adhered to planar membrane. (*E*) The background fluorescence of free Eth. (*F*) A cell becomes detectably labeled by Eth 562 s after acidification (*arrow* and *arrowhead F* on conductance record). Increases in conductance and movement of Eth evolved much more slowly for BHA-PI than for HA-WT cells. Less Eth entered the BHA-PI cells in accord with the low g_{hd} compared with fully open pores with HA-WT cells. Bar, 50 μm.

sion occurs through hemifusion. This study establishes that a lipid-anchored ectodomain of HA induces hemifusion.

GPI-linked proteins have been observed to sequester within caveolae (Anderson et al., 1992) and form complexes rich in glycolipids and cholesterol (Sargiacomo et al., 1993). However, sequestration may have occurred only after cross-linking these proteins (Mayor et al., 1994). In fact, fluorescence recovery after photobleaching indicates that GPI-HA and wt-HA have the same high mobile fractions and similar lateral mobilities, consistent with free diffusion within membranes (Kemble et al., 1993). Hence, the evidence suggests that GPI-HA is not sequestered in microdomains. Furthermore, any enrichments of lipids around GPI-HA should be limited to the outer cell leaflet. Because the outer leaflet is excluded from the hemifusion diaphragm (Fig. 9), even if lipid enrichment did occur, pore formation should not be affected.

Hemifusion, without Full Fusion, Occurs between BHA-PI Cells and Target Membranes

The probe R18 (and DiI) transferred from the outer leaflet of RBCs to BHA-PI cells under fusogenic conditions, whereas the inner leaflet and aqueous dyes remained confined. It is unlikely that small fusion pores formed, preventing movement of aqueous fluorescent dyes as occurred for wt-HA–mediated fusion (Zimmerberg et al., 1994). If they did, the inner leaflet probe should have spread. It is topologically required that lipids of the contacting leaflets as well as all integral membrane proteins

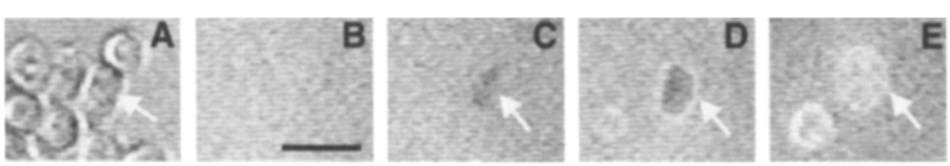

Figure 8. Pattern of fluorescence changes upon hemifusion of BHA-PI cells to rhoPE-containing planar bilayers indicates the hemifusion diaphragm is extended. Only the selected area of interest on the planar membrane is shown. Bright-field (*A*) and fluorescence images (*B*) before acidification of a relevant area of a planar membrane. The arrow (*A*) marks the first cell that will hemifuse. (*C*) A slightly darkened area formed underneath the hemifusing cell (*arrow*), indicating clearing of rhoPE from the proximal, cell-facing, monolayer of the planar membrane by unlabeled cell membrane. (*D*) The onset of rhoPE dequenching appeared as a donut, a brighter perimeter surrounding the dark area (*arrow*). For this panel, eight sequential frames were averaged to help make the donut pattern of dequenching apparent. (*E*) Further dye spread into this cell led to an increase of fluorescence intensity over the whole cell area (*arrow*). The shape of the fluorescence changed from irregular (*C*) to circular (*E*) apparently due to the tension of the planar membrane. Hemifusion of a second nearby cell is also apparent. Bar, 25 μm.

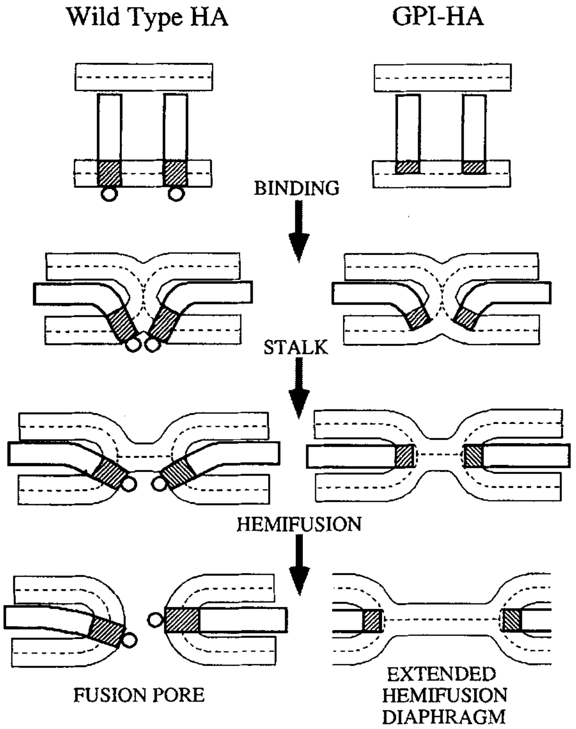

Figure 9. Elastic coupling model for HA-mediated membrane fusion. (*Left*) wt-HA. The ectodomain of HA leads to stalk formation and hemifusion. The TM, mechanically coupled to the ectodomain, is reoriented and generates stress within the hemifusion diaphragm, leading to fusion pore formation. (*Right*) GPI-HA. The bending of the ectodomain does not transmit stresses to the hemifusion diaphragm. Fusion pores do not form and the diaphragm enlarges.

be excluded from the hemifusion diaphragm. Because the diaphragm must be lipidic, any fusion pores within the diaphragm must also be lipidic. The membrane probe FM4-64 included in an inner leaflet should sift through, moving along the walls of the pore providing continuity between the RBC and BHA-PI cell inner leaflets. We cannot, however, exclude the possibility that a few transient pores formed, without one ever irreversibly opening. But if repetitive flickering over an extended period occurred, detectable amounts of both membrane, FM4-64, and aqueous, Eth dyes should have transferred: indeed, when HA-WT cells exhibited recurrent flickering (without full pore opening) over prolonged time with planar membranes, Eth was observed to transfer from the bottom solution to cytosol (data not shown). Also, spread of rhoPE from planar membranes into HA-WT cells was detected during an extended flickering stage, suggesting that an observable quantity of FM4-64 should also move if flickering was protracted. Thus, it is unlikely that extended pore flickering occurred between RBCs and BHA-PI cells. In spite of occasional destabilizations of hemifusion diaphragms, the evidence is against the formation of bona fide fusion pores with BHA-PI cells. In contrast, full fusion occurred between RBCs and HA-WT cells: all the fluorescent dyes used to label RBCs (R18 [and DiI] within the outer monolayer leaflets, FM4-64 [and FM1-43] within the inner leaflets, and aqueous dyes [CF and Eth] within RBCs) transferred to HA-WT cells.

Full fusion also occurred between planar membranes and HA-WT cells; hemifusion, but not full fusion, proceeded with BHA-PI cells. Fusion pores were always observed before detecting movement of rhoPE from the planar membrane to HA-WT cells. In contrast, for BHA-PI cells lipid dye moved before any electrical activity (Fig. 5), unambiguously establishing the phenomenon of HA ectodomain–induced hemifusion. The electrical response subsequent to hemifusion was dramatically different from that characteristic of pore formation. While g_{hd} increased, fusion pores did not form with BHA-PI cells.

Hemifusion Diaphragms Tend to Enlarge

The hemifusion diaphragm between BHA-PI cells and RBCs should consist of a single lipid bilayer and peripheral proteins, as the integral membrane proteins as well as cytoskeletal elements should be excluded. Lipid bilayers lyse when subjected to about one-half the isotropic tension required to lyse RBC membranes (Evans et al., 1976), making it possible that in the osmotic swelling experiments (Fig. 4) lysis occurred preferentially within the diaphragm. But this dissimilarity would be compensated if RBCs swelled more readily than BHA-PI cells because the inner leaflet of the RBC would then be stretched, whereas the BHA-PI cell would not. In fact, BHA-PI cells did not visibly swell (data not shown) or lyse in response to the stress (Fig. 4 *D*). Therefore, while it is not possible to calculate the area of the hemifusion diaphragm from the osmotic lysis experiments, it can be estimated to have an area as high as a few percent of the total RBC membrane area assuming equal compressibility of the two regions. The diaphragm appears to reach an equilibrium area soon after hemifusion: the same percentage of BHA-PI cells became labeled by aqueous dye independent of whether osmotic lysis was generated at 2 or 45 min after acidification (while we consider it unlikely, it is possible that there are thousands of localized, nonextended, hemifusion sites). That the diaphragm does not grow indefinitely is explained by simple geometric considerations (Kozlov et al., 1989). In RBC to BHA-PI hemifusion, lipids of the contacting leaflets are displaced from the hemifused to the nonhemifused region. An excess of lipids thus accumulates in the outer leaflets of the two cells compared with the inner leaflets. As a consequence, the outer leaflets are compressed, the inner leaflets stretched. Growth in the area of the hemifusion diaphragm accentuates this mismatch, limiting the size of the diaphragm.

Fluorescence and capacitance measurements show that with planar membranes as target the diaphragms may become much larger than with RBCs (Fig. 8). This is expected. When hemifused to planar membranes, the outer cell leaflet is continuous with the contacting, top planar bilayer leaflet, which in turn is connected to the supporting torus. Similarly, the noncontacting, bottom leaflet of the planar bilayer is connected to the torus. Both leaflets of the bilayer are under the same tension, on the order of 1–3 dyne/cm (Needham and Haydon, 1983), which pulls them into the torus. Because these tensions are equal, the areas of the hemifused and nonhemifused portions of the cell are the same at equilibrium, assuming the membrane proteins and cytoskeletal elements excluded from the hemifusion diaphragm do not prevent its expansion. This was borne out in practice: the average capacitance of BHA-PI cells not incorporated into the hemifusion diaphragm, 8 pF, was one-half that of the wild-type cells, 17 pF, indicating that half of the BHA-PI cell membrane constituted the hemifusion diaphragm. This remarkable numerical agreement with the theoretical expectation may be somewhat fortuitous. Uncertainties in quantifying g_{hd} (see Materials and Methods) could have caused the capacitances of the nonhemifused regions of BHA-PI cells to be underestimated. Additionally, these capacitances could be measured only when g_{hd} became large, which may have occurred more readily for fully extended diaphragms. If the case, the measured capacitances of nonhemifusion regions would have been selected from experiments in which diaphragms became exceptionally large. While it is not definitive that half of the BHA-PI cell membrane incorporated into the hemifusion diaphragm, it is clear that this diaphragm developed a large area. Tension acting on an extended area of the diaphragm could contribute to the observed increases in g_{hd} after hemifusion and movement of Eth into BHA-PI cells via a permeable diaphragm (Fig. 7).

Localized Intermediate Structure Leading to Hemifusion

The very fact that hemifusion diaphragms become large limits the possibilities for the initial connecting structure in HA-mediated fusion. If protein gap–junction-like structures (Almers, 1990) or inverted micelles (Bentz et al., 1990) were the initial connecting structures, the lipids and proteins would have to undergo tortuous rearrangements for the diaphragm to enlarge. Also, as the large diaphragm is probably a single bilayer, the initial structure should be able to readily expand into an extended bilayer. A "stalk–pore" model (Kozlov et al., 1989) satisfies these requirements (Fig. 9). However, because monolayer leaflets must peel apart to form a stalk, it is possible that energetically unfavorable interstitial hydrophobic spaces form, referred to as void volumes, and preclude the stalk from expanding into a large structure (Siegel, 1993*b*). The large diaphragms observed with both a model (planar bilayer) membrane and a biological (RBC) membrane show that, in fact, void energies are not of major consequence.

Does HA-mediated Membrane Fusion Proceed through Hemifusion?

The conformational changes that the ectodomain of fully constructed wt-HA undergoes appear to be the same as those of the ectodomain in the form of GPI-HA (Kemble et al., 1993) or of ectodomain obtained by bromelain cleavage of HA (Doms et al., 1985; White and Wilson, 1987). The similarities in conformational changes indicate that wt-HA should be capable of inducing hemifusion. But it is still unknown whether wt-HA induces hemifusion before pore formation.

With wt-HA, a fusion pore usually fully enlarged after a short stage of flickering. Lipids should diffuse freely between fused membranes connected by flickering pores having nS conductances (Tse et al., 1993; Zimmerberg et al., 1994) as observed in our experiments. But, lipid dye spread was not observed until after full enlargement (Fig. 5). It is thus clear that membrane continuity is established well before lipid dye is observed to spread. This is expected because lipid dye moves relatively slowly, and a sufficient amount of dye must enter the fused cells for its fluorescence to exceed the background fluorescence of the planar membrane. Electrical measurements, however, are sufficiently sensitive to capture the formation of fusion pores with millisecond time resolution, that is, without time delays. Therefore, hemifusion could have occurred before a pore formed and dye spread not detected until after pore formation. Our working hypothesis is that the ectodomain of the fully constructed wt-HA induces hemifusion, and the transmembrane domain and perhaps the cytosolic region induce the formation of pores in the hemifusion diaphragm.

Separate Domains of HA May Control Individual Steps in Fusion: Elastic Coupling between HA Domains May Lead to Pore Formation within Hemifused Diaphragms

In the bound state (Fig. 9, *binding*) at neutral pH, each HA monomer is 13.5 nm long with its fusion peptide (not shown) 10 nm from the target membrane into which it will insert (Wilson et al., 1981). In response to low pH, the ectodomain of HA would have to reconfigure approximately parallel to the HA-containing membrane to reduce the relatively long distances between the membranes (Stegmann et al., 1990; Guy et al., 1992; Siegel, 1993*a*). These conformational changes, including the insertion of the hydrophobic fusion peptide of HA into the HA-containing and target membranes (Harter et al., 1989; Stegmann et al., 1991; Zimmerberg et al., 1993; Weber et al., 1994; Wharton et al., 1995), probably induces a stalk structure that connects membranes (Fig. 9, *stalk*). The initial stalk would expand and the distal leaflets of the original membranes would then meet to form a single bilayer (Fig. 9, *hemifusion*). At this point the membranes would be in a state of hemifusion. Integral membrane proteins, including wt-HA, would remain confined to the nonhemifused regions, unable to enter the target membrane without disturbing the diaphragm.

We propose that mechanical coupling between the ectodomain and the transmembrane domain of HA (TM) is responsible for pore formation within the hemifusion diaphragm. In this elastic coupling model, bending of the HA ectodomain pulls on the TM and cytoplasmic regions of HA (Wilschut and Bron, 1993). This coupling would tend to force the TM more parallel to the plane of the membrane (Fig. 9, *stalk* to *hemifusion*) which would generate stresses on the diaphragm and disturb the configurations of its lipids. Additionally, low pH causes profound reorientations of α helices of the HA2 subunit (Carr and Kim, 1993; Bullough et al., 1994). These large scale movements should be transmitted to the TM and hence to the hemifusion diaphragm. Stresses on the diaphragm would be relieved by fusion pore formation (Fig. 9). The hydrophilic cytoplasmic tails might also destabilize the diaphragm. Independent of the precise intermediates, if hemifusion occurs at all, TMs would be excluded from the hemifusion diaphragm. The configuration shown in Fig. 9 (*hemifusion*) would still occur and pore formation would proceed as described above. The role of the cytoplasmic tail appears to be less important than the transmembrane domain. Infectious virions lacking the cytoplasmic tail of HA were released (Jin et al., 1994) and truncating or deleting the cytoplasmic region of HA did not dramatically reduce formation of syncytia (Simpson and Lamb, 1992), implying that fusion activity does not require the cytoplasmic tail.

The experiments with BHA-PI cells indicates that the hemifusion diaphragm has a propensity to enlarge. We envision that pores form only while the diaphragm has not appreciably expanded, in other words while its diameter is comparable to the length of the TM and cytoplasmic tail. If the diaphragm enlarges too much, the HA trimers will not act cooperatively. Also, bending distortions will not be focused into a small region.

The movement of the GPI-linked ectodomain is not mechanically coupled to the noncontacting leaflet. The GPI anchor can enter the target membrane without perturbing the hemifusion diaphragm. Thus, large movements of the ectodomain could be accommodated without severely bending or stressing the membrane. Additionally, the region where the ectodomain of HA is linked to GPI would be flexible (Tartakoff and Singh, 1992), perhaps more so than the corresponding region within wt-HA; this would aid movements without producing stresses. Thus, the hemifusion diaphragm would form and enlarge, without formation of fusion pores. Generating cells with molecularly engineered HA, constructed with altered or deleted TMs and cytoplasmic tails, in conjunction with functional study could determine the role of domains in pore formation.

We are grateful to Dr. W. D. Niles for useful discussions and help with digitizing video images. Ms. S. Brener provided excellent technical assistance. Dr. S. Goodman generated Figure 9. We thank Drs. L. V. Chernomordik, W. D. Niles, and S. V. Popov for critical and considered readings of the manuscript.

Supported by National Institutes of Health GM 27367 and AI 22470.

Received for publication 10 May 1995 and in revised form 24 July 1995.

References

Ahkong, Q. F., J.-P. Desmazes, D. Georgescauld, and J. A. Lucy. 1987. Movement of fluorescent probes in the mechanism of cell fusion induced by poly(ethylene glycol). *J. Cell Sci.* 88:389–398.

Almers, W. 1990. Exocytosis. *Annu. Rev. Physiol.* 52:607–624.

Anderson, R. G. W., B. A. Kamen, K. G. Rothberg, and S. W. Lacey. 1992. Potocytosis: sequestration and transport of small molecules by caveolae. *Science (Wash. DC).* 255:410–411.

Bentz, J., H. Ellens, and D. Alford. 1990. An architecture for the fusion site of influenza hemagglutinin. *FEBS Lett.* 276:1–5.

Betz, W. J., F. Mao, and G. S. Bewick. 1992. Activity-dependent fluorescent staining and destaining of living vertebrate motor nerve terminals. *J. Neurosci.* 12:363–375.

Bullough, P. A., F. M. Hughson, J. J. Skehel, and D. C. Wiley. 1994. Structure of influenza haemagglutinin at the pH of membrane fusion. *Nature (Lond.).* 371:37–43.

Carr, C. H., and P. S. Kim. 1993. A spring-loaded mechanism for the conformational change of influenza hemagglutinin. *Cell.* 73:823–832.

Chernomordik, L. V., G. B. Melikyan, and Yu. A. Chizmadzhev. 1987. Biomembrane fusion: a new concept derived from model studies using two interacting planar lipid bilayers. *Biochim. Biophys. Acta.* 906:309–352.

Chernomordik, L., A. Chanturiya, J. Green, and J. Zimmerberg. 1995. The hemifusion intermediate and its conversion to complete fusion: regulation by membrane composition. *Biophys. J.* 69: 922–929.

Doms, R. W. 1993. Protein conformational changes in virus-cell fusion. *Methods Enzymol.* 221:61–72.

Doms, R. W., A. Helenius, and J. M. White. 1985. Membrane fusion activity of the influenza virus hemagglutinin (the low pH-induced conformational change). *J. Biol. Chem.* 260:2973–2981.

Ellens, H., J. Bentz, and F. C. Szoka. 1985. H^+- and Ca^{2+}-induced fusion and destabilization of liposomes. *Biochemistry.* 24:3099–3106.

Ellens, H., S. Doxsey, J. S. Glenn, and J. M. White. 1989. Delivery of macromolecules into cells expressing a viral membrane fusion protein. *Methods Cell Biol.* 31:155–176.

Guy, H. R., S. R. Durell, C. Schoch, and R. Blumenthal. 1992. Analyzing the fusion process of influenza hemagglutinin by mutagenesis and molecular modeling. *Biophys. J.* 62:113–115.

Harter, C., P. James, T. Bachi, G. Semenza, and J. Brunner. 1989. Hydrophobic binding of the ectodomain of influenza hemagglutinin to membranes occurs through the "fusion peptide". *J. Biol. Chem.* 264:6459–6464.

Helm, C. A., J. N. Israelachvili, and P. M. McGuiggan. 1992. Role of hydrophobic forces in bilayer adhesion and fusion. *Biochemistry.* 31:1794–1805.

Heuser, J., Q. Zhu, and M. Clarke. 1993. Proton pumps populate the contractile vacuoles of *Dictyostelium amoebae. J. Cell Biol.* 121:1311–1327.

Jin, H., G. P. Leser, and R. A. Lamb. 1994. The influenza virus hemagglutinin cytoplasmic tail is not essential for virus assembly or infectivity. *EMBO (Eur. Mol. Biol. Organ.) J.* 13:5504–5515.

Kalderon, N., and N. B. Gilula. 1979. Membrane events involved in myoblast fusion. *J. Cell Biol.* 81:411–425.

Kemble, G. W., Y. I. Henis, and J. M. White. 1993. GPI- and Transmembrane-anchored influenza hemagglutinin differ in structure and receptor binding activity. *J. Cell Biol.* 122:1253–1265.

Kemble, G. W., T. Danieli, and J. M. White. 1994. Lipid-anchored influenza hemagglutinin promotes hemifusion, not complete fusion. *Cell.* 76:383–391.

Kozlov, M. M., S. L. Leikin, L. V. Chernomordik, V. S. Markin, and Yu. A. Chizmadzhev. 1989. Stalk mechanism of membrane fusion. *Eur. Biophys. J.* 17:121–129.

Leventis, R., J. Gagne, N. Fuller, R. P. Rand, and J. R. Silvius. 1986. Divalent cation induced fusion and lateral segregation in phosphatidylcholine-phosphatidic acid vesicles. *Biochemistry.* 25:6978–6987.

LePecq, J.-B., and C. Paoletti. 1967. Fluorescent complex between ethidium bromide and nucleic acids. *J. Mol. Biol.* 27:87–106.

Lindaü, M., and E. Neher. 1988. Patch-clamp techniques for time-resolved capacitance measurements in single cells. *Pflügers Arch. Eur. J. Physiol.* 411: 137–146.

Lucy, J. A., and Q. F. Ahkong. 1986. An osmotic model for the fusion of biological membranes. *FEBS Lett.* 199:1–11.

MacDonald, R. 1990. Characteristics of self-quenching of the fluorescence of lipid-conjugated rhodamine in membranes. *J. Biol. Chem.* 265:13533–13539.

Mayor, S., K. G. Rothberg, and F. R. Maxfield. 1994. Sequestration of GPI-anchored proteins in caveolae triggered by cross-linking. *Science (Wash. DC).* 264:1948–1951.

Melikyan, G. B., W. D. Niles, M. E. Peeples, and F. S. Cohen. 1993*a*. Influenza hemagglutinin-mediated fusion pores connecting cells to planar membranes: flickering to final expansion. *J. Gen. Physiol.* 102:1131–1149.

Melikyan, G. B., W. D. Niles, and F. S. Cohen. 1993*b*. Influenza virus hemagglutinin-induced cell-planar bilayer fusion: quantitative dissection of fusion pore kinetics into stages. *J. Gen. Physiol.* 102:1151–1170.

Melikyan, G. B., W. D. Niles, and F. S. Cohen. 1995*a*. The fusion kinetics of influenza hemagglutinin expressing cells to planar bilayer membranes is affected by HA density and host cell surface. *J. Gen. Physiol.* 106.

Melikyan, G. B., W. D. Niles, V. A. Ratinov, M. Karhanek, J. Zimmerberg, and F. S. Cohen. 1995*b*. Comparison of transient and successful fusion pores connecting influenza hemagglutinin expressing cells to planar membranes. *J. Gen. Physiol.* 106.

Morris, S. J., D. P. Sarkar, J. M. White, and R. Blumenthal. 1989. Kinetics of pH-dependent fusion between 3T3 fibroblasts expressing influenza hemagglutinin and red blood cells. *J. Biol. Chem.* 264:3972–3978.

Nanavati, C., V. S. Markin, A. F. Oberhauser, and J. M. Fernandez. 1992. The exocytotic fusion pore modeled as a lipidic pore. *Biophys. J.* 63:1118–1132.

Needham, D., and D. A. Haydon. 1983. Tensions and free energies of formation of "solventless" lipid bilayers. *Biophys. J.* 41:251–257.

Neher, E. 1974. Asymmetric membranes resulting from the fusion of two black lipid bilayers. *Biochim. Biophys. Acta.* 373:327–336.

Palade, G. E. 1975. Intracellular aspects of the process of protein synthesis. *Science (Wash. DC).* 189:347–358.

Papahadjopoulos, D., S. Nir, and S. Ohki. 1971. Permeability properties of phospholipid membranes: effect of cholesterol and temperature. *Biochim. Biophys. Acta.* 266:561–583.

Pinto da Silva, P., and M. L. Nogueira. 1977. membrane fusion during secretion. A hypothesis based on electron microscope observation of *Phytophthora Palmivora* zoospores during encystment. *J. Cell Biol.* 73:161–181.

Rogers, G. N., and J. C. Paulson. 1983. Receptor determinants of human and animal influenza virus isolates: differences in receptor specificity of the H3 hemagglutinin based on species of origin. *Virology.* 127:361–373.

Sargiacomo, M., M. Sudol, Z. Tang, and M. P. Lisanti. 1993. Signal transducing molecules and glycosyl-phosphatidylinositol-linked proteins form a caveolin-rich insoluble complex in MDCK cells. *J. Cell Biol.* 122:789–807.

Siegel, D. P. 1993*a*. Modeling protein-induced fusion mechanisms: insight from the relative stability of lipidic structures. *In* Viral Fusion Mechanisms. J. Bentz, editor. CRC Press, Inc., Boca Raton, FL. pp. 475–512.

Siegel, D. P. 1993*b*. Energetics of intermediates in membrane fusion: comparison of stalk and inverted micellar intermediate mechanisms. *Biophys. J.* 65: 2124–2140.

Simpson, D. A., and R. A. Lamb. 1992. Alterations to influenza virus hemagglutinin cytoplasmic tail modulate virus infectivity. *J. Virol.* 66:790–803.

Song, L., Q. F. Ahkong, D. Georgescauld, and J. A. Lucy. 1991. Membrane fusion without cytoplasmic fusion (hemi-fusion) in erythrocytes that are sub-

jected to electrical breakdown. *Biochim. Biophys. Acta.* 1065:54–62.
Spruce, A. E., A. Iwata, J. M. White, and W. Almers. 1989. Patch clamp studies of single cell-fusion events mediated by a viral fusion protein. *Nature (Lond.).* 342:555–558.
Stegmann, T., and A. Helenius. 1993. Influenza virus fusion: from models toward mechanisms. *In* Viral Fusion Mechanisms. J. Bentz, editor. CRC Press, Inc., Boca Raton, FL. 89–111.
Stegmann, T., J. M. White, and A. Helenius. 1990. Intermediates in influenza induced membrane fusion. *EMBO (Eur. Mol. Biol. Organ.) J.* 9:4231–4241.
Stegmann, T., J. M. Delfino, F. M. Richards, and A. Helenius. 1991. The HA2 subunit of influenza hemagglutinin inserts into the target membrane prior to fusion. *J. Biol. Chem.* 266:18404–18410.
Steinhauer, D. A., N. K. Sauter, J. J. Skehel, and D. C. Wiley. 1992. Receptor binding and cell entry by influenza virus. *In* Seminars in Virology. Saunders Scientific Publications, Academic Press, Ltd., London, UK. 91–100.
Stenger, D. A., and S. W. Hui. 1986. Kinetics of ultrastructural changes during electrically induced fusion of human erythrocytes. *J. Membr. Biol.* 93:43–53.
Tartakoff, A. M., and N. Singh. 1992. How to make glycoinositol phospholipid anchor. *TIBS (Trends Biochem. Sci.).* 17:470–473.
Tse, F. W., A. Iwata, and W. Almers. 1993. Membrane flux through the pore formed by a fusogenic viral envelope protein during cell fusion. *J. Cell Biol.* 121:543–552.
Weber, T., G. Paesold, C. Galli, R. Mischler, G. Semenza, and J. Brunner. 1994. Evidence for H^+-induced insertion of influenza hemagglutinin HA2 N-terminal into viral membrane. *J. Biol. Chem.* 269:18353–18358.
Wharton, S. A., L. J. Cadler, R. W. H. Ruigrok, J. J. Skehel, D. A. Steinhauser, and D. C. Wiley. 1995. Electron microscopy of antibody complexes of influenza virus haemagglutinin in the fusion pH conformation. *EMBO (Eur. Mol. Biol. Organ.) J.* 14:240–246.
White, J. M. 1992. Membrane fusion. *Science (Wash. DC).* 258:917–924.
White, J. M. 1994. Fusion of influenza virus in endosomes: role of the hemagglutinin. *In* Cellular Receptors for Animal Viruses. E. Wimmer, editor. Cold Spring Harbor Laboratory, Cold Spring Harbor, NY. 281–301.
White, J. M., and I. A. Wilson. 1987. Anti-peptide antibodies detect steps in a protein conformational change: low-pH activation of the influenza virus hemagglutinin. *J. Cell Biol.* 105:2887–2896.
Wiley, D. C., and J. I. Skehel. 1987. The structure and function of the hemagglutinin membrane glycoprotein of influenza virus. *Annu. Rev. Biochem.* 56: 365–394.
Wilschut, J., and R. Bron. 1993. The influenza virus hemagglutinin: membrane fusion activity in intact virions and reconstituted virosomes. *In* Viral Fusion Mechanisms. J. Bentz, editor. CRC Press, Inc., Boca Raton, FL. 133–161.
Wilson, I. A., J. J. Skehel, and D. C. Wiley. 1981. Structure of the haemagglutinin membrane glycoprotein of influenza virus at 3 A° resolution. *Nature (Lond.).* 289:366–373.
Zimmerberg, J., S. S. Vogel, and L. V. Chernomordik. 1993. Mechanisms of membrane fusion. *Annu. Rev. Biophys. Biomol. Struct.* 22:433–466.
Zimmerberg, J., R. Blumenthal, D. P. Sarkar, M. Curran, and S. J. Morris. 1994. Restricted movement of lipid and aqueous dyes through pores formed by influenza hemagglutinin during cell fusion. *J. Cell Biol.* 127:1885–1894.